THE INTERNATIONAL JOURNAL OF MEDICAL ROBOTICS AND COMPUTER ASSISTED SURGERY
Int J Med Robotics Comput Assist Surg 2010; **6**: 368–375.
Published online 22 July 2010 in Wiley Online Library (wileyonlinelibrary.com) **DOI:** 10.1002/rcs.347

ORIGINAL ARTICLE

Multi-objective optimization of end-to-end sutured anastomosis for robot-assisted surgery

Ying Liu[1]
Shuxin Wang[1]*
S. Jack Hu[2]

[1]*School of Mechanical Engineering, Tianjin University, Tianjin 300072, People's Republic of China*

[2]*Department of Mechanical Engineering, College of Engineering, University of Michigan, Ann Arbor, MI 48109-2125, USA*

*Correspondence to: Shuxin Wang, School of Mechanical Engineering, Tianjin University, Tianjin 300072, People's Republic of China.
E-mail: shuxinw@tju.edu.cn

Accepted: 11 June 2010

Abstract

Background Due to differences in surgical operations between free-hand and robot-assisted vessel anastomosis, there exist new challenges in applying the manipulation criteria of free-hand surgery to robot-assisted surgery in order to guarantee successful completion of the surgical procedure.

Methods A mathematical model is established to optimize the process variables in vessel anastomosis. The distance between entry point and cross-section, suture tension and the number of individual sutures are selected as design variables. The allowable range of suture tension and the difference between longitudinal stresses of vessel tissue on transverse sections are used as the objective functions. Simulation experiments are carried out to obtain the allowable range of suture tension and tissue stress distribution, based on numerical analysis.

Results For a vessel in anastomosis with 4 mm diameter, a larger distance between the entry point and the cross-section and/or more sutures can result in less tissue deformation and a tighter joint between the two vessel ends. The allowable range of suture tension is a function of the number of individual sutures and increases with the decrease of the distance between entry point and cross-section. The optimal designs providing the suture configuration of distance between entry point and cross-section and the number of individual sutures are presented in the case that the performance of robot-assisted anastomosis can be guaranteed without strong control of suture tension.

Conclusions The work provides meaningful results for the optimal design of the suturing procedure in robot-assisted vascular anastomosis when the robotic system does not allow tactile feedback. Copyright © 2010 John Wiley & Sons, Ltd.

Keywords robot-assisted surgery; vessel anastomosis; multi-objective optimization; blood vessel engineering; Pareto solution

Introduction

Vascular anastomosis is one of the most essential but difficult tasks in surgery. It is required in many surgical procedures involving blood vessels. There is no consensus about the history of vascular surgical techniques, but the most commonly recognized milestones are briefly summarized below. Vascular ligation was the only vascular procedure until a vascular reconstruction was reported by Lambert in 1762 (1,2). It was in 1899 that end-to-end anastomosis in humans was first performed by Kummell (3). In the following decades, many

Copyright © 2010 John Wiley & Sons, Ltd.

suture techniques were developed, such as absorbable vs nonabsorbable sutures, continuous vs interrupted stitches. During the end of the nineteenth and the early twentieth century, various non-suture techniques were experimentally introduced into vascular surgery. Based on the materials used, the non-suture techniques can be categorized into five groups: rings, clips, adhesives, stents and laser welding (4). However, the sutured technique is still the most popularly used method in vascular anastomosis.

With the development of medical robot technology, high precision and accuracy can be obtained in vascular surgery, such as in microvascular reconstruction, by scaling down motion (5–9). In particular, surgeon movement scaling is very useful to perform thin vessel suture. In robot-assisted surgery, the surgeon performs surgical tasks through audio, visual and physical instruments to see, interact and communicate with the patient (10). Robot-assisted surgery induces an indirect contact between hand and internal tissue, consequently impairing the haptic perception capability which enables the surgeon to measure tissue properties and control action by exerting appropriate force. For a robotic system without tactile feedback, the surgeon can estimate the applied force through visual feedback by observing the tissue deformation, although there is still limited eye–hand coordination in currently available robotic systems (11,12), namely the ability of the vision system to coordinate the information received from the visual instrument and to control, guide and direct the hand in the accomplishment of a surgical task.

Because of the difference of the operation format between free-hand surgery and robot-assisted surgery, there exist new challenges in guaranteeing the success of the surgical procedure in robot-assisted vascular anastomosis. In free-hand surgery, vascular anastomosis is accomplished by the surgeon observing vessel tissue deformation and controlling the suture tension through eye–hand coordination. Application of the manipulation criteria to robot-assisted vascular anastomosis requires understanding the surgery process, establishing quality evaluation criteria, assessing variables that influence the quality of surgery, and determining the relationship between the variables and the quality of the surgery. Furthermore, the quality of the operation can be enhanced by optimization of the variables.

In order to ensure quality of anastomosis, Liu *et al*. (13) investigated the vessel tissue stress distribution in the process of operation and presented the minimal and maximal allowable tension loaded on a vessel, using the finite elements method. However, there are other factors, such as the number of individual sutures and the distance between the entry point and cross-section of the vessel, which influence the quality of anastomosis as well as suture force and vessel stress. For example, sufficient sutures are necessary to ensure that the vessel anastomosis is free from blood leakage, but excessive sutures are time-consuming and increase the risk of infection. Also, strong suture force is needed to prevent blood leakage but too big a force probably causes damage to the vessel tissue. Clearly, there is a need for optimization in the number of sutures and sutures force, but, there is a lack of systematic attempts to optimize robot-assisted vascular anastomosis, which is the aim of this study.

This study investigates the physical process of end-to-end silk-sutured vascular anastomosis. A mathematical model, including optimization variables, multi-objective functions and constraint conditions, is established to describe the optimization problem in robot-assisted vascular anastomosis. Simulation experiments are arranged to obtain the allowable range of suture tension and distribution of tissue stress, based on the finite elements model of the surgery process. The relationship between objective functions and variables is achieved by analysing the experimental data. A Pareto optimal solution is presented, which is supplied to surgeons for selection according to applications. Using the optimal design, the performance of anastomosis, which is executed by a robot system with incorporated tactile feedback, can be guaranteed without a strong control of suture tension.

Materials and Methods

Process of end-to-end anastomosis

The vascular anastomosis technique consists of end-to-end, end-to-side and side-to-side joining (3). For simplicity, this study uses end-to-end anastomosis of equal-sized vessels as an example. Based on observations of manual anastomosis operations, an anastomosis process can be decomposed into three major surgery tasks: vessel exposure and mobilization; creation of a transverse arteriotomy; and suturing (14,15).

In the operations, the surgeon needs to decide the proper type of instruments, the distance between entry point and cross-section, and the exact number of individual sutures according to the diameter and wall thickness of the vessel. It is also required that the sutures be placed on the circumference of the vessel by equal spacing so that the wall stress is uniform after anastomosis. Therefore, the factors involved in the process of end-to-end vessel anastomosis are the physical properties of the blood vessel, vessel diameter, vessel wall thickness, diameter of the needle used, diameter of the suture, physical properties of the suture, distance between the entry point and cross-section, suture tension, and the number of individual sutures.

Among these factors, vessel diameter, vessel wall thickness and the physical properties of the vessel are characteristics associated with the patient, while the type of needle and suture are chosen by the surgeon according to the diameter and wall thickness of the vessel. These factors combined help to determine the selection of the needle, suture and number of individual sutures and their placements. Accordingly, they are adopted as parameters in the mathematical model for optimization design of vessel anastomosis. The diameter and wall thickness of

Copyright © 2010 John Wiley & Sons, Ltd.

DOI: 10.1002/rcs

Table 1. Parameters in the anastomosis model

Parameter		Value
Suture	Diameter	0.07(0.05) mm
	Tensile strength	1.37 N
	Density	900 kg/m^3
	Young's modulus	1.32–1.42 GPa
	Poisson ratio	0.35
Needle	Diameter	0.05 mm
Vessel diameter		4 mm
Vessel thickness		0.4 mm

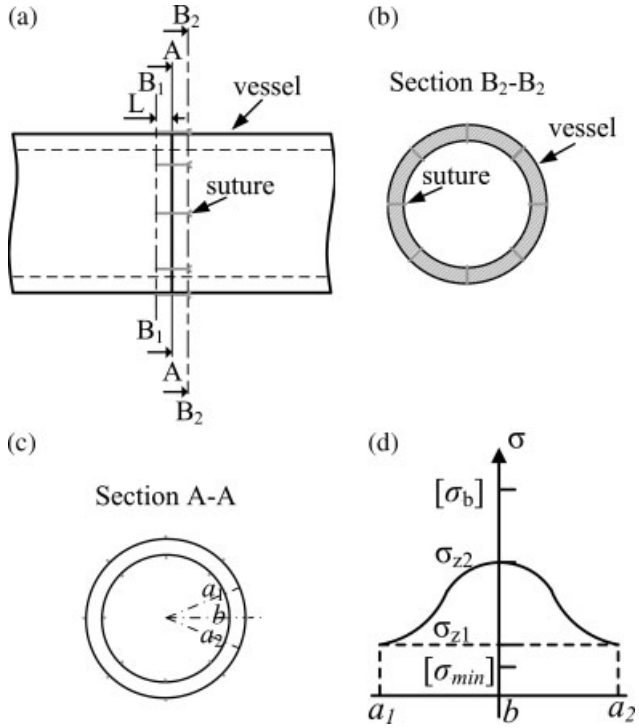

Figure 1. Arrangement of the sutures and distance between entry point and cross-section on vessels: (a) front view; (b) cutaway view (Section B_2–B_2); (c) cross-section of vessel (Section A–A); (d) distribution curve of longitudinal stress; σ_{z1} is the longitudinal stress at points a_1 and a_2; σ_{z2} is the longitudinal stress at point b

the vessel are selected as 4 mm and 0.4 mm, respectively (16). Accordingly, the type of suture and needle is selected as 7-0 (15). The values of these parameters are shown in Table 1 (3,14–16). The distance between the entry point and the cross-section, suture tension and the number of individual sutures are decided by the surgeon to guarantee the quality of surgery. Therefore, they are selected as design variables in the optimization model.

Design variable

Figure 1 shows the arrangement of the sutures and the distance between the entry point and the cross-section of the vessel. Let N be the number of individual sutures, L the distance between entry point and cross-section and T the suture tension, respectively. The design variable can be represented as:

$$\boldsymbol{x} = [x_1, x_2, x_3]^T = [N, L, T]^T \tag{1}$$

Various types of techniques are available for the anastomosis of blood vessels. As for the perpendicular end-to-end anastomosis by means of an over-and-over suture with interrupted stitches studied in this work, suture methods of the two ends of the divided vessels can be two stay-stitches, three stay-stitches or four stay-stitches (3). Hence, the value of N can be 4, 6, 8, 9, 10, 12, 14, 15 or 16 when the vessel diameter is 4 mm. The distance between entry point and cross-section may be in the range 0.4–0.6 mm and it is transformed to a discrete value due to convenience of modelling the anastomosis process (3,14,15). Suture tension is designed as 0–1.3 N according to the tensile strength of suture. The values of L, N and T can be shown as:

$$\begin{aligned} x_1 &= N \in \{4, 6, 8, 9, 10, 12, 14, 15, 16\} \\ x_2 &= L \in \{0.4, 0.5, 0.6\} \\ x_3 &= T \subset (0.0, 1.3) \end{aligned} \tag{2}$$

Objective function

The basic clinical requirements for a successful anastomosis procedure include the following: (a) no breaking of thread material; (b) no tissue injury; (c) no blood leakage; and (4) inclusion of the entire thickness of the vessel wall and achieving intima-to-intima coaptation. According to Liu *et al.* (13), the maximum principal stress of vessel tissue induced by suture tension should be smaller than the allowable tensile strength to prevent tissue injury. On the other hand, the longitudinal tissue stress induced by suture tension should be larger than that by the normal blood pressure without regard to the blood viscosity, to avoid blood leakage. This can be represented as follows:

$$\begin{aligned} \sigma_1 &\le [\sigma_\mathrm{b}] \\ \sigma_\mathrm{z} &\ge [\sigma_\mathrm{min}] \end{aligned} \tag{3}$$

where σ_1 is the maximum principal stress of the vessel, $[\sigma_\mathrm{b}]$ is the allowable tensile strength obtained from the material test, σ_z is the longitudinal stress induced by suture tension and $[\sigma_\mathrm{min}]$ is the longitudinal stress at normal blood pressure.

Accordingly, the tension loaded on a suture should be in the range $([T_\mathrm{min}], [T_\mathrm{max}])$ to avoid both tissue injury and blood leakage, where $[T_\mathrm{min}]$ and $[T_\mathrm{max}]$ are the minimal and maximal allowable suture tensions, respectively. For a surgeon, the bigger the difference between $[T_\mathrm{max}]$ and $[T_\mathrm{min}]$, the more advantageous the manipulation of the surgery and the lower the skill needed for the surgery. Consequently, one objective function of the mathematical model for optimization of vessel anastomosis can be represented as to maximize the following objective:

$$f_1(x) = \Delta T = ([T_\mathrm{max}] - [T_\mathrm{min}]) \tag{4}$$

Copyright © 2010 John Wiley & Sons, Ltd.

For convenience, the distribution of longitudinal stress on the inner wall of the transverse section can be presented by the curve in Figure 1c when the suture tension is $[T_{\min}]$. Let σ_{z1} be the minimal longitudinal stress, σ_{z2} the maximal longitudinal stress and $\Delta\sigma_z$ the difference between σ_{z2} and σ_{z1}. For vessel tissue, the smaller the $\Delta\sigma_z$, the more advantageous the healing of the blood vessel. Consequently, the other objective function of the mathematical model for optimization of vessel anastomosis is to minimize:

$$f_2(x) = \Delta\sigma_z = (\sigma_{z2} - \sigma_{z1}) \tag{5}$$

At the same time, σ_{z1}, σ_{z2} and σ_1 must be in the range (13,17,18). That is to say:

$$\begin{aligned} [\sigma_{\min}] \le \sigma_{z1} \le [\sigma_b] \\ [\sigma_{\min}] \le \sigma_{z2} \le [\sigma_b] \\ [\sigma_{\min}] \le \sigma_1 \le [\sigma_b] \end{aligned} \tag{6}$$

Thus, the mathematical model of optimization of end-to-end vascular anastomosis can be expressed as follows:

$$\begin{aligned} &\min F(x) = \min\{-f_1(x), f_2(x)\} \\ &f_1(x) = \Delta T = ([T_{\max}] - [T_{\min}]) \\ &f_2(x) = \Delta\sigma_z = (\sigma_{z2} - \sigma_{z1}) \\ &x = [N, L, T]^T \in D \subset R^3 \\ &\text{s.t. } [\sigma_{\min}] - \sigma_{z1} \le 0 \\ &[\sigma_b] - \sigma_{z1} \ge 0 \\ &[\sigma_{\min}] - \sigma_{z2} \le 0 \\ &[\sigma_b] - \sigma_{z2} \ge 0 \\ &[\sigma_{\min}] - \sigma_1 \le 0 \\ &[\sigma_b] - \sigma_1 \ge 0 \\ &[T_{\max}] - [T_{\min}] \ge 0 \end{aligned} \tag{7}$$

Simulation experiment

The magnitude and distribution of wall stress of on the vessel are determined by the number of individual sutures, the distance between the entry point and the cross-section, and suture tension. However, it is impossible to obtain analytical solutions, due to the complexity of the constitutive equation and the non-linearity of the vessel material. In addition, the results of existing experimental studies do not provide three-dimensional stress–strain distributions in the vessel wall. Hence finite element modelling (FEM) analysis is used to obtain the magnitude and distribution of tissue stress.

Table 2. Design matrix of vessel anastomosis optimization

Run	1	2	3	4	5	6	7	8	9
x_1	4			6			8		
x_2 (mm)	0.4	0.5	0.6	0.4	0.5	0.6	0.4	0.5	0.6
x_3 (N)	0–1.3								
Run	10	11	12	13	14	15	16	17	18
x_1	9			10			12		
x_2 (mm)	0.4	0.5	0.6	0.4	0.5	0.6	0.4	0.5	0.6
x_3 (N)	0–1.3								
Run	19	20	21	22	23	24	25	26	27
x_1	14			15			16		
x_2 (mm)	0.4	0.5	0.6	0.4	0.5	0.6	0.4	0.5	0.6
x_3 (N)	0–1.3								

The vessel anastomosis processes are simulated using ABAQUS. The finite element model of vessel anastomosis is set up by analysing the mechanical process of anastomosis (13), where the constant parameters are listed in Table 1. Meshes of varying density can be generated in different parts of the vessel with the desired accuracy and efficiency. The element type selected is C3D8R, an eight-node linear isoparametric hexahedral element with reduced integration and hourglass control. The FE simulation of the vessel anastomosis process indicates that the magnitude and the precise locations of strains and stresses in the structure are caused by the applied tension on the suture. The suture tension that affects the quality of vessel anastomosis is obtained by the simulation.

Simulation experiments organized by the design of experiments (DOE) method are arranged to gain the response of tissue stress vs the variables. The relationship between the objective functions and process variables is extracted from experimental data. Full factorial design is adopted for the simulation experiment. T is a continuous variable, and L and N are discrete variables in the finite element model of the surgical process. Note that each combination of variable level is labelled with a different run number, so there are $3 \times 9 = 27$ runs in the experiments. Table 2, the design matrix, lists the settings of the three variables for all the 27 runs, based on equation (2). For instance, in run 7, $x_1 = 8$, $x_2 = 0.4$ and $x_3 \in (0, 1.3)$ means that the number of individual sutures and the distance between entry point and cross-section are evaluated as 8 and 0.4 mm, respectively, and the suture tension is controlled within the range 0–1.3 N.

Results

According to the tissue stress analysis of simulation experiments, the value of $[T_{\min}]$ is larger than that of $[T_{\max}]$ when the number of individual sutures is 4,

Copyright © 2010 John Wiley & Sons, Ltd.

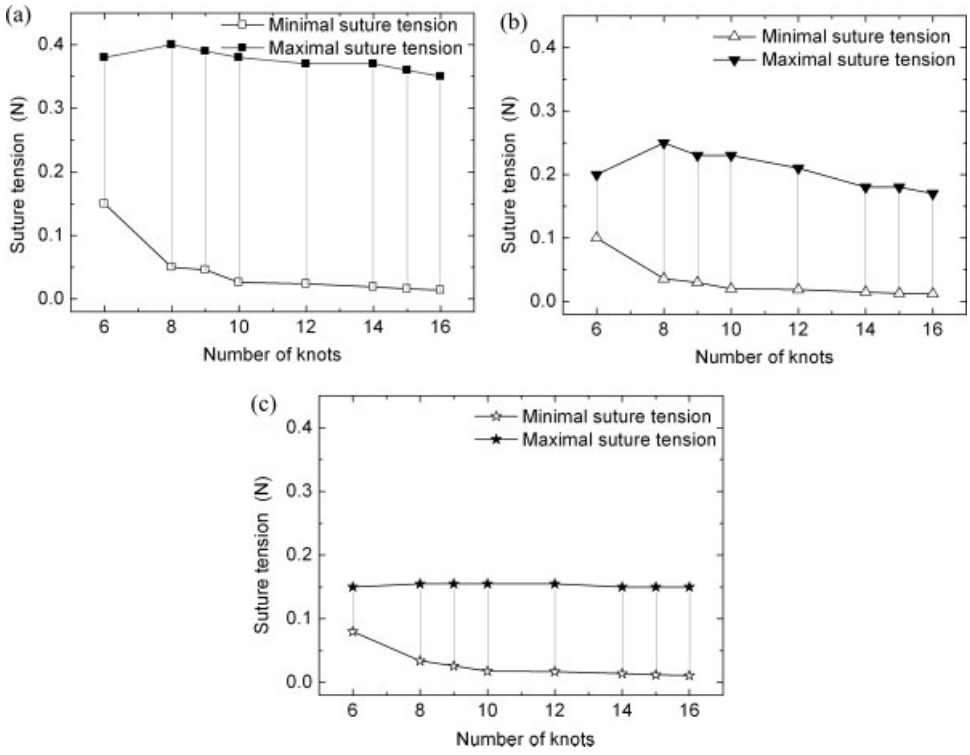

Figure 2. Allowable suture tension at different levels of L and N: (a) $L = 0.4$ mm; (b) $L = 0.5$ mm; and (c) $L = 0.6$ mm

which is lacking in basic physical meaning. Therefore, the minimal number of individual sutures for end-to-end vessel anastomosis is 6 when the vessel diameter is 4 mm at normal blood pressure.

Allowable suture tension

Figure 2a–c illustrates the simulation results of the minimal and maximal allowable suture tensions with different numbers of individual sutures (6, 8, 9, 10, 12, 14, 15 and 16) in the conditions that the distance between the entry point and the cross-section is 0.4, 0.5 and 0.6 mm, respectively. As shown in Figure 2a, the maximal allowable suture tension has a peak value of 8 sutures when the distance between the entry point and the cross-section is 0.4 mm, and the minimal allowable suture tension decreases anti-logarithmically and simultaneously with the increase of the number of sutures. Similar features of the allowable suture tension against the number of individual sutures are demonstrated in Figure 2b, c. Besides, it can be seen from Figure 2 that 6, 8, 10 and 16 can be regarded as the key points of N in each level of L. Thus, the value of the minimal and maximal allowable suture tensions for the key points of N with different levels of L are listed and compared in Figure 3.

As can be seen from Figure 3, as for each given N, the maximal allowable suture tension $[T_{max}]$ decreases rapidly with the increase of the distance between entry point and cross-section. However, the minimal allowable suture tension $[T_{min}]$ decreases with a speed slower than that of the former $[T_{max}]$ with the increase of the distance

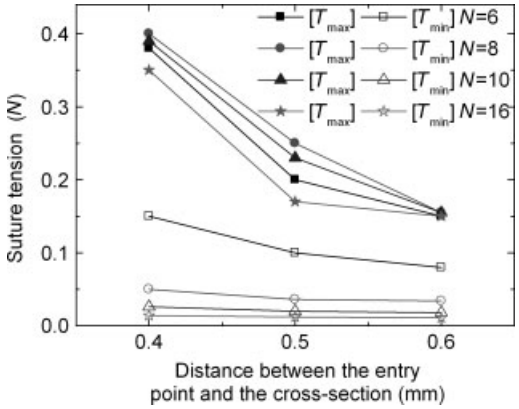

Figure 3. Allowable suture tension at different levels of L with $N = 10$

between entry point and cross-section when the number of individual sutures is 6. It becomes almost constant when the number of individual sutures is >6, such as 8 or 10.

Distribution of longitudinal stress

Figure 4 illustrates the comparison of σ_{z1} and σ_{z2} at different levels of L and N when the suture tension equals $[T_{min}]$. According to Liu *et al.* (13), σ_{z1} amounts to $[\sigma_{min}]$ at this time. As can be seen from Figure 4, σ_{z2} decreases with the increase of L in the condition of each given N. Meanwhile, when L is a given level, σ_{z2} also decreases with the increase of N until it becomes nearly constant when the number of individual sutures reaches 10. the

Copyright © 2010 John Wiley & Sons, Ltd.

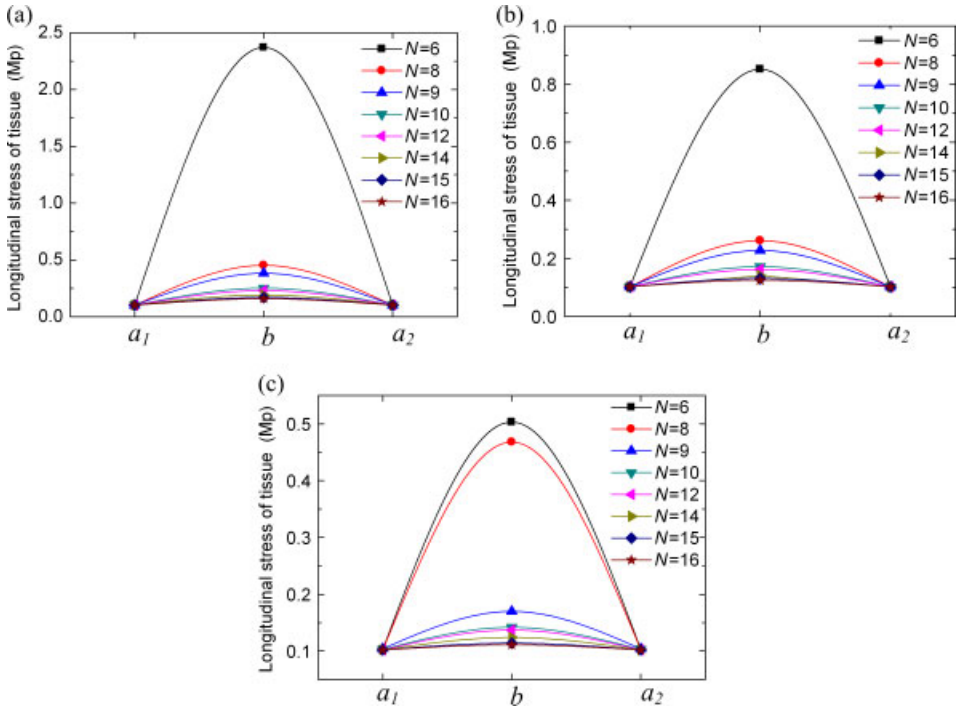

Figure 4. Longitudinal stress of tissue on the inner wall of the cross-section with different levels of L and N: (a) $L = 0.4$ mm; (b) $L = 0.5$ mm; and (c) $L = 0.6$ mm

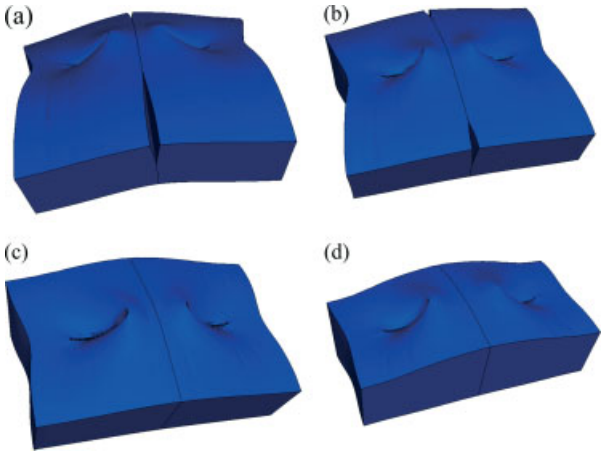

Figure 5. Comparison of tissue deformation with $L = 0.60$. mm: (a) $N = 6$; (b) $N = 8$; (c) $N = 12$; and (d) $N = 16$

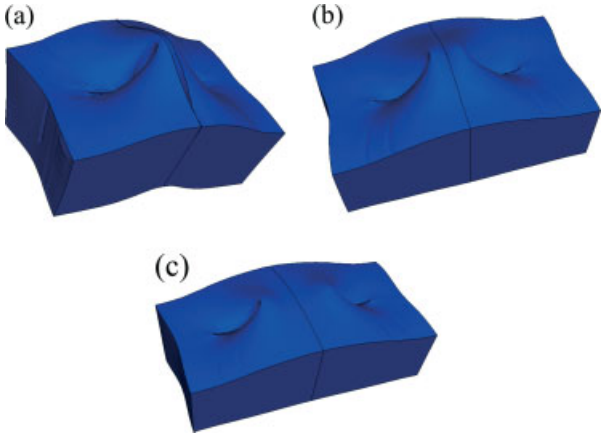

Figure 6. Comparison of tissue deformation with $N = 16$: (a) $L = 0.4$ mm; (b) $L = 0.5$ mm; and (c) $L = 0.6$ mm

conclusion that σ_{z2} is mostly influenced by L when the number of individual sutures is not less than 10 can be deduced from the experimental data presented in Figure 4.

Figures 5 and 6 illustrate a comparison of tissue deformation at different levels of L and N. As can be seen from the figures, the larger L and N are, the less the tissue deformation, the tighter the join between the two vessel ends and the more advantageous the tissue reconstruction.

Pareto optimal solution

Figure 7 plots the values of the objective functions against the distance between entry point and cross-section and the number of individual sutures. It can be seen that $f_1(x)$ and $f_2(x)$ have different features and convergent direction. The influence of variables on the allowable range of suture tension is shown graphically in Figure 7a. The allowable range of suture tension increases with the decrease of the distance between entry point and cross-section. It also increases with the number of individual sutures when N is at a low level. However, for a high level of N, the increase of the sutures just causes a small reduction in the allowable range of suture tension. Meanwhile, the figure shows that the distance between the entry point and the cross-section has a larger effect on $f_1(x)$ than does the number of individual sutures. Figure 7b illustrates the influence of the variables on $f_2(x)$. In general, increasing the distance between the entry

Copyright © 2010 John Wiley & Sons, Ltd.

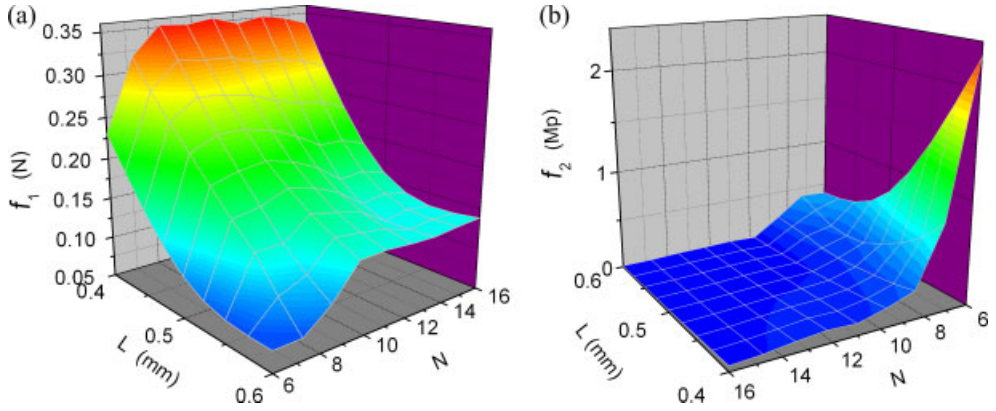

Figure 7. Relationship between the objective functions f_1 (a), f_2 (b), and the variables

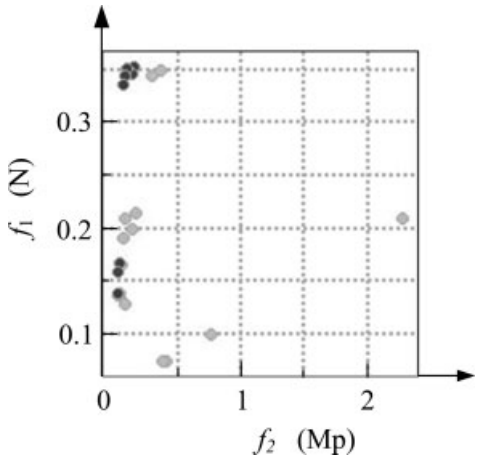

Figure 8. Pareto optimal set for end-to-end vessel anastomosis

Table 3. Pareto optimal design for end-to-end vessel anastomosis

L (mm)	n	f_1 (N)	f_2 (Mp)
0.4	10	0.354	0.15
0.4	12	0.346	0.128
0.4	14	0.351	0.089
0.4	15	0.344	0.067
0.4	16	0.336	0.056
0.5	15	0.167	0.029
0.5	16	0.158	0.023
0.6	16	0.139	0.009

point and the cross-section and the number of individual sutures tends to improve the outcome of anastomosis. Also, the effect on $f_2(x)$ of the distance between the entry point and the cross-section is smaller than that of the number of individual sutures, which is inverse with $f_1(x)$. In addition, there are certain interaction effects between L and N.

The vessel anastomosis design is formulated as a multi-objective non-linear mathematical programming model of both discrete and continuous variables. The presence of multiple objectives usually gives rise to a set of optimal solutions, largely known as Pareto optimal solutions (19). A Pareto set is represented by a set of solutions, such that when one moves from one solution to any other, at least one objective function improves while the others worsen. The Pareto solution shown in Figure 8 is presented for the optimization problem, where the horizontal and vertical axes are the allowable range of suture tension and the minimal difference between the longitudinal stresses of the vessel wall on the cross-section. The highlighted points (dark grey) are the Pareto optimal solution and the corresponding results are shown in Table 3.

Discussion

With the development of medical robotic technology, there exist several differences in the surgical operations between free-hand and robot-assisted vascular anastomosis. The new challenge is how to apply the manipulation criteria of free-hand surgery to robot-assisted surgery in order to guarantee successful completion of the surgical procedure. The robotic surgery can be formulated as a multi-objective optimization problem, since the surgeon can perform the surgical procedure with quantitative information supplied by robotic systems. In this paper, a multi-objective non-linear mathematical programming model has been set up for the first time to describe the process of end-to-end vessel anastomosis. The distance between entry point and cross-section, suture tension and the number of individual sutures were selected as design variables. The allowable range of suture tension and the differences between longitudinal stresses of vessel tissue on the transverse section are used as the objective functions of the mathematical model for optimization of vessel anastomosis.

For a robotic system without tactile feedback, it is useful to know the suture approach, which arranges the distance between entry point and cross-section and number of individual sutures and gives the range of suture tension to guarantee the performance of vessel anastomosis. By means of the simulation experiments, the minimal and maximal allowable suture tensions are achieved to perform the anastomosis successfully with different levels of the distance between entry point and cross-section and the number of individual sutures. Taking

Copyright © 2010 John Wiley & Sons, Ltd.

as an example a vessel with 4 mm diameter, the value of $[T_{\min}]$ is larger than that of $[T_{\max}]$ when the number of individual sutures is four. That is to say, if four sutures are used to join the two vessels, blood leakage may be unavoidable, even if the suture is loaded a tensile force large enough to damage the vessel tissue. Therefore, the minimal number of individual sutures for end-to-end vessel anastomosis should be six for a vessel with 4 mm diameter at normal blood pressure. However, the minimal N may be far from the best choice because the high suture tension when $N = 6$ is likely to damage the vessel tissue, and this risk can be weakened by increasing the number of individual sutures, N. Besides, more sutures are needed to avoid blood leakage for the cases of hypertension (viz. high blood pressure). Therefore, it is necessary to further analyse the influences of design variables on the two objective functions.

It can be seen from Figure 7 that the influences of the design variables L and N on the two objective functions are quite different. In detail, the influence of the number of individual sutures on the allowable range of suture tension is much smaller than that of the distance between entry point and cross-section. However, the influence of the number of individual sutures on the difference between longitudinal tissue stress on the transverse section is much larger than that of the distance between entry point and cross-section. In addition, there are interaction effects between the design variables. Moreover, a larger distance between entry point and cross-section and/or more sutures results in less tissue deformation and a tighter joint, and is thus more advantageous for tissue reconstruction. On the other hand, both a smaller distance between entry point and cross section and a larger allowable range of suture tension are more advantageous for surgical manipulation.

Based on the comparison of allowable suture tension and longitudinal stress on the cross-section, a set of optimal solutions is obtained, providing the optimal suture configuration of distance between entry point and cross-section and number of individual sutures. Following the optimal result, the surgeon can get a good suture without strong control of suture tension. As an example, the first optimization solution means the allowable range of suture tension and minimal difference of the longitudinal vessel stress on cross-section will be 0.354 N and 0.15 Mpa when the distance between the entry point and the cross-section and the number of individual sutures is 0.4 mm and 10, respectively, for a vessel with 4 mm diameter. The allowable lower and upper limits of suture tension can be found from Figure 2 and the minimal difference of the longitudinal stress of vessel wall on the cross-section can be obtained on condition that the suture tension equals to the allowable lower limit.

In other words, the result is meaningful for the design of an optimal suturing procedure in robot-assisted anastomosis when the robotic system does not allow tactile feedback. The method introduced in this paper can be extended to end-to-end anastomosis with other vessel sizes and other suture techniques (e.g. end-to-side anastomosis).

Acknowledgements

This research was supported by the NSFC (Grant No. 50925520) and the National High-Tech R&D Programme of China (863 Programme, Grant No. 2007AA04Z247).

References

1. Liapis CD, Balzer K, Benedetti-Valentini F, *et al*. *Vascular Surgery*. Springer -Verlag Berlin Heidelberg 2007.
2. Ascher E, Hollier LH, Strandness DE Jr, *et al*. *Haimovici's Vascular Surgery*. Wiley-Blackwell: Chichester, 2003.
3. Rutherford RB. Cronenwett JL, Gloviczki P, *et al*. *Vascular Surgery*. Elsevier Saunders: Philadelphia, 2005.
4. Zeebregts CJ, Heijmen RH, Van Den Dungen JJ, *et al*. Non-suture methods of vascular anastomosis. *Br J Surg* 2003; **90**(3): 261–271.
5. Zamorano L, Li Q, Jain S, Kaur G. Robotics in neurosurgery: state of the art and future technological challenges. *Int J Med Robot Comput Assist Surg* 2004; **1**(1): 7–22.
6. Belsley SJ, Byer A, Ballantyne GH. MIRA and the future of surgical robotics. *Int J Med Robot Comput Assist Surg* 2006; **2**(1): 98–103.
7. Puangmali P, Althoefer K, Seneviratne LD, *et al*. State-of-the-art in force and tactile sensing for minimally invasive surgery. *IEEE Sens J* 2008; **8**(3–4): 371–381.
8. Preusche C, Hirzinger G. Haptics in telerobotics – current and future research and applications. *Visual Comput* 2007; **23**(4): 273–284.
9. Wang S, Ding J, Yun J, Li Q, Han B. A Robotic system with force feedback for micro-surgery. Proceedings of the 2005 IEEE International Conference on Robotics and Automation, April 2005; Barcelona, Spain; 199–204.
10. Speich JE, Rosen J. Medical robotics. In *Encyclopedia of Biomaterials and Biomedical Engineering*, Bowlin GL, Wnek G (eds). Marcel Dekker: New York, 2004; 983–993.
11. Stallkamp J, Schraft RD. A technical challenge for robot-assisted minimally invasive surgery: precision surgery on soft tissue. *Int J Med Robot Comput Assist Surg* 2005; **1**(2): 48–52.
12. Howe RD, Matsuoka Y. Robotics for surgery. *Annu Rev Biomed Eng* 1999; **1**: 211–240.
13. Liu Y, Wang S, Hu SJ, Qiu W. Mechanical analysis of end-to-end silk-sutured anastomosis for robot-assisted surgery. *Int J Med Robot Comput Assist Surg* 2009; **5**(4): 444–451.
14. Liu X. *Histology and Embryology*. People's Medical Publishing House: Beijing, 1994.
15. Guo W, Xu M. *Basic Surgical Operation*. Scientific and Technical Documents Publishing House: Beijing, 1993.
16. Fung YC. *Biomechanics: Mechanical Properties of Living Tissues*. Springer-Verlag: Berlin, 1983.
17. Patel DJ, Vaishnav RN. *Basic Hemodynamics and Its Role in Disease Processes*. University Park Press: Baltimore, MD, 1980.
18. Fung YC. *Biomechanics: Motion, Flow, Stress, and Growth*. Springer-Verlag: New York, 1990.
19. Huang P, Meng YG. *Optimal Theories and Methods*. Tsinghua University Press: Beijing, 2009.

Copyright © 2010 John Wiley & Sons, Ltd.